STM JOURNALS

Journal of
Polymer & Composites

ISSN: 2321-2810 (Online)
ISSN: 2321-8525 (Print)
Volume 14, Issue 3, 2026
DOI (Journal): 10.37591/JoPC

https://journals.stmjournals.com/jopc

Research JoPC

Hybrid Numerical–Artificial Neural Network Study of Chemically Reactive MHD Nanofluid Flow Incorporating Thompson–Troian Slip and Stefan Blowing

S. Harinath Reddy[1], R. Chandra Sekhar Reddy[2], Aruna Ganjikunta[3], P. Ramakrishna Reddy[4], P. Chandra Reddy[5*]

Abstract

Boundary layer behaviour in chemically reactive nanoliquid is significantly affected by surface conditions, magnetic fields, heat and mas transfer mechanisms. However, the combined impact of Stefan blowing and nonlinear Thompson–Troian slip under inclined magnetic fields remains mostly unexplored, particularly in mixed convection flows. In this research work, the flow of a chemically reactive nanoliquid over a permeable surface is investigated by considering the Troian slip, inclined magnetic fields, Stefan blowing, and mixed convection. The Buongiorno nanofluid model is utilized to incorporate Brownian motion and thermophoretic diffusion. By similarity transformetions, the governed expressions are simplified into ordinary differentials and solved using a hybrid approach, such as shooting and an Artificial Neural Network (ANN) technique. The ANN guesses show sturdy pact with numerical outcomes, yielding a maximum error of 6.113×10^{-10} for skin friction, Nusselt, and Sherwood numbers. Findings indicate that Stefan blowing decreases fluid velocity while increasing the layer of temperature. Brownian motion and thermophoresis significantly enhance thermal and solutal profiles, whereas surface slip mitigates these effects. The inclined magnetic field reduces flow velocity and skin friction due to the Lorentz force but boosts heat and mass transfer rates. Mixed convection enhances momentum exchange at the wall, while the chemical reaction reduces nanoparticle concentration.

Keywords: Inclined magnetic field, mixed convection, chemically reactive nanofluid, Thompson-Torian slip, Stefan blowing, Numerical-ANN Approach.

***Author for Correspondence**
P. Chandra Reddy

1Assistant Professor, Department of Mathematics, Annamacharya University, Rajampet, Andhra Pradesh, India
2Assistant Professor, Department of Mathematics, Rajeev Gandhi Memorial College of Engineering and Technology, Nerawada, X' Roads, Nandyala, Andhra Pradesh, India
3Associate Professor, Department of Mathematics, Malla Reddy (MR) Deemed to be University, Secunderabad, Hyderabad, Telangana, India
4Professor, Department of Mathematics, PBR Visvodaya Institute of Technology and Science, Kavali, Andhra Pradesh, India
5*Assistant Professor, Department of Mathematics, Annamacharya University, Rajampet, Andhra Pradesh, India

Received Date: April 11, 2026
Accepted Date: April 23, 2026
Published Date: May 15, 2026

Citation: S. Harinath Reddy, R. Chandra Sekhar Reddy, Aruna Ganjikunta, P. Ramakrishna Reddy, P. Chandra Reddy. Hybrid Numerical–Artificial Neural Network Study of Chemically Reactive MHD Nanofluid Flow Incorporating Thompson–Troian Slip and Stefan Blowing. Journal of Polymer & Composites. 2026; 14(3): 409–425p.

INTRODUCTION

Nanofluids have been raised with recognition as a critical-edge mode of working because of their greater competences compared with heat transfer of conventional base fluids. Solid nanoparticles, typically smaller than 100 nm, are distributed into base liquids like water, oil, or ethylene glycol to form these fluids. Nanofluids are attractive for use in solar energy systems, electronic cooling, and biomedical thermal applications because of this mixture's notable increase in thermal conductivity. In order to improve the thermal conductivity of traditional heat transfer fluids by dispersing nanoscale solid particles, Choi and Eastman [1] initially proposed nanofluids. Das *et al*. [2] later demonstrated that verified that temperature and nanoparticle properties had a significant impact on

thermal enhancement through experimental research. Buongiorno [3] offered a physical foundation for nanoparticle transport, identified and studied Brownian motion and thermophoresis as the two main mechanisms in convective nanofluid flows. Further research revealed abnormally high thermal conductivity in fluids based on nanoparticles [4], and Xuan and Li [5] demonstrated that nanofluids greatly enhance convective heat transfer efficiency. Recent research has extended the application of nanofluids to intricate boundary layer flow situations, such as multi-phase systems and porous media [6–10].

Magnetohydrodynamics (MHD) and mixed convection studies significantly impact transport processes in electrically conducting fluids. The interplay of Lorentz force and buoyancy effects changes velocity and heat transport and the boundary layer structure, and they are used in energy systems, materials processing, nanofluid-based biomedical applications, liquid metal cooling, and electronic thermal management. For instance, magnetically induced nanofluid flow with wall mass transfer effects through a similarity framework was developed by Kandasamy *et al*. [11]. Their research produces a modelling technique for conducting nanofluid boundary layer transport. Later, Yadav *et al*. [12] examined both internal and boundary heat source effects on nano liquids. The impact of magnetic forces on heat transfer flow behaviour has been highlighted in recent studies that have addressed MHD nanofluid flows under various conditions in the presence of convection [13–18]. The address by Aydin and Kaya [19] gives magnetically driven diverse convective flow along a porous vertical surface. Their findings revealed that stronger buoyancy and suction escalate the shear stress coefficient, whereas blowing reduces it in the presence of these combined effects. The buoyancy-driven flow in magnetically controlled porous media under radiative effects and morphology-dependent features, with the help of ANN-assisted numerical technique, is investigated by Raza *et al*. [20]. Recent research has demonstrated the effectiveness of intelligent models for forecasting heat and flow behavior by analyzing magnetically controlled convection in complex fluid systems using neural network-based techniques [21–23].

Slip boundary conditions and Stefan blowing are particularly significant in micro- and nano-scale flows, where the traditional no-slip assumption is inadequate. Thompson and Troian [24] introduced a nonlinear slip model that links slip velocity to local shear stress, capturing molecular-scale interactions at fluid–solid interfaces. Experiments have confirmed the occurrence of velocity slip at hydrophobic surfaces, especially in microchannels is studied by Tretheway and Meinhart [25]. MHD flows with slip conditions show complex solution behavior, including multiple branches and altered heat and mass transfer characteristics [26-28]. Mohanaphriya and Chakraborty [29] demonstrated that chemical interactions and various slip mechanisms significantly influence entropy generation in magnetically driven nanofluid flow in the presence of radiative effects, being a crucial factor in thermal irreversibility. Nonlinear slip circumstances dramatically alter heat transfer and flow behavior in chemically reactive non-Newtonian hybrid nanofluids over curved geometries, as discussed by Algarni [30]. Many researchers [31-35] investigated Stefan blowing effects on nanofluid flow and reported that it significantly alters the boundary layer development and transport rates. Albaqami [36] expressions that ANN works well for solving tricky nonlinear problems related to nanofluid flow. Abdal *et al*. [37] study investigates the magnetohydrodynamic (MHD) pour of a non-Newtonian liquid in excess expanding expanse, incorporating properties of warm and mass transport, substance responses, and bioconvection owing to motile microorganisms. Shettar *et al*. [38] offerings an in-depth analysis of how water immersion affects the technical possessions of glass fiber–nanoclay–epoxy combinations. Arunachalam *et al*. [39] describes he integration of MWCNTs with jute, kenaf, and glass fibers in a hybrid composite matrix significantly improves technical possessions such as flexural concentration and hardness.

Although wide-ranging studies done on nanofluid heat and mass transfer, Stefan blowing and Thompson–Troian slip on chemically reactive nanoliquid flow over a permeable surface have not been comprehensively investigated within a unified boundary-layer framework. The novelty is summarized as follows:

- A unified boundary-layer formulation is developed for chemically reactive nanoliquid flow over a permeable plate by simultaneously incorporating nonlinear Thompson–Troian slip, Stefan blowing, mixed convection, and an inclined magnetic field.
- The analysis explicitly accounts for magnetic field inclination, rather than assuming a purely transverse magnetic field, providing a more realistic description of magnetohydrodynamic flow control.
- Nonlinear Thompson–Troian slip conditions are utilized to describe near-wall transport behavior that extends beyond traditional no-slip or linear slip models.
- A combined numerical–Artificial Neural Network (ANN) approach is presented, where precise numerical solutions obtained through bvp4c are used to train an ANN for the efficient prediction.

MATHEMATICAL MODEL

The study examines a steady, two-dimensional boundary-layer flow of a viscous, incompressible, and chemically reactive nanofluid over a permeable flat plate. The plate is oriented along the x-axis, while the y-axis is perpendicular to the surface, extending into the fluid domain (refer to Fig. 1). The flow is restricted to the xy-plane. The physical assumptions and boundary characteristics of the mathematical model are outlined as follows:

- At the plate surface (y=0), a nonlinear Thompson–Troian slip condition is applied to the tangential velocity, whereas Stefan blowing/suction regulates the normal velocity.
- A uniform powered magnetic boundary (B_0) is applied at an inclination angleα , generating a Lorentz force in the streamwise direction.
- Mixed convection results from thermal and solutal buoyancy effects.
- Nanoparticle transport adheres to the Buongiorno model, incorporating Brownian motion and thermophoresis.

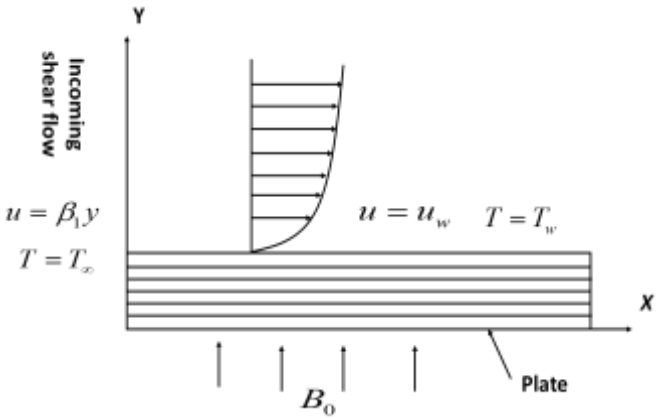

Figure 1. Physical Configuration of Problem

Under these conditions, the governing equations are represented by Eqs. (1)–(4).

$$\frac{\partial u}{\partial x}+\frac{\partial v}{\partial y}=0 \tag{1}$$

$$u\frac{\partial u}{\partial x}+v\frac{\partial u}{\partial y}=\upsilon\frac{\partial^2 u}{\partial y^2}-\frac{\sigma B_0^2}{\rho_f}\sin^2\alpha\, u + \frac{1}{\rho_f}\left\{\rho_f\beta_T\left(1-C_\infty\right)\left(T-T_\infty\right)-\left(\rho_p-\rho_f\right)\left(C-C_\infty\right)\right\}g \tag{2}$$

$$u\frac{\partial T}{\partial x}+v\frac{\partial T}{\partial y}=\alpha\frac{\partial^2 T}{\partial y^2}+\frac{(\rho c)_p}{(\rho c_p)_f}\left[D_B\frac{\partial C}{\partial y}\frac{\partial T}{\partial y}+\frac{D_T}{T_\infty}\left(\frac{\partial T}{\partial y}\right)^2\right] -\frac{1}{(\rho C_p)_f}\frac{\partial q_r}{\partial y}+\frac{\mu}{(\rho C_p)_f}\left(\frac{\partial u}{\partial y}\right)^2+\frac{\sigma B_0^2}{(\rho c_p)_f}\sin^2\alpha\, u^2 \tag{3}$$

$$u\frac{\partial C}{\partial x}+v\frac{\partial C}{\partial y}=D_B\frac{\partial^2 C}{\partial y^2}+\frac{D_T}{T_\infty}\frac{\partial^2 T}{\partial y^2}-k_1(C-C_\infty) \tag{4}$$

With boundary conditions

$$u=\gamma\left(1-\xi\frac{\partial u}{\partial y}\right)^{-0.5},\ v=\frac{-D_B}{(1-C_w)}\frac{\partial C}{\partial y},\ T=T_w,\ C=C_w \text{ at } y=0 \tag{5}$$

$$u=u_\infty(y)=\beta_1 y,\ T=T_\infty,\ C=C_\infty \text{ as } y\to\infty \tag{6}$$

SIMILARITY VARIABLES

$$\eta=\frac{y}{L}\left(\frac{x}{L}\right)^{-\frac{1}{3}},\ \theta=\frac{T-T_\infty}{T_w-T_\infty},\ \psi=\upsilon\left(\frac{x}{L}\right)^{\frac{2}{3}}f(\eta),\ \phi=\frac{C-C_\infty}{C_w-C_\infty} \tag{9}$$

where $u=\frac{\partial\psi}{\partial y},\ v=-\frac{\partial\psi}{\partial x}$

Using (6)–(8) in the boundary layer Eq. (2), energy Eq. (3) and concentration Eq. (4) the following equation are obtained.

$$3f'''+2ff''-f'^2-3M\sin^2\alpha f'+\lambda(\theta-Ri\phi)=0 \tag{10}$$

$$(3+4Rd)\theta''+2\Pr f\theta'+3Nb\phi'\theta'+3Nt\theta'^2+3Ecf''^2+3MEc\sin^2\alpha f'^2=0 \tag{11}$$

$$3\phi''Nb+3Nt\phi''+Le\{2f\phi'-3Kr\phi\}=0 \tag{12}$$

with boundary conditions:

$$2f=\frac{3S}{Le}\phi',\ f'=\delta(1-\beta f'')^{-0.5}f'',\theta=1,\phi=1 \tag{13}$$

$$f''=1,\theta=0,\phi=0 \tag{14}$$

The analysis of the physical problem includes the evaluation as follows

$$\mathrm{Re}_x^{\frac{1}{2}}Cfx=f''(0) \tag{15}$$

$$\mathrm{Re}_x^{\frac{-1}{2}}Nu=-\theta'(0) \tag{16}$$

$$\mathrm{Re}_x^{\frac{-1}{2}}Sh=-\phi'(0) \tag{17}$$

ANN ANALYSIS

The Artificial Neural Network (ANN) model, illustrated in the figure, was trained using the Levenberg–Marquardt optimization technique. To assess the accuracy of the model, the Mean Squared Error (MSE), the Coefficient of Determination (R), and the error rate (ER) were used. Their mathematical formulations (i = 1, 2, 1,2, 3,… N) are given as

$$R = \left[1 - \frac{\sum_i \left(Y_{true,i} - Y_{pred,i} \right)^2}{\sum_i (Y_{true,i})^2} \right]^{0.5}$$

$$ER(\%) = \left(\frac{Y_{pred}}{Y_{true}} \times 100 \right)$$

A MATLAB program was created and processed the data using ANN techniques. The dataset for training the ANN was extracted from data generated using the shooting method in MATLAB. By using input as well as output variables the ANN has been developed. A total of 450 data points were used, out of 70% is used for training, 15% each for validation and testing, utilizing the *divider and* function.

RESULTS AND DISCUSSION

In this study, the effect of Stefan blowing, Thompson-Troian slip and an inclined magnetic field is combined to investigate the flow of chemically reactive nanoliquid across a permeable wall by using hybrid computation methods such as bvp4c and ANN approach. Engineering metrics of these profiles are depicted in Fig. 2-14.

Fig.2 (a) demonstrates the significant impact of the blowing parameter S on the velocity profile. Increasing S reduces the velocity field near the surface, reflecting the physical effect of fluid injection. Figures 2(b) and 2(c) illustrate the variation of temperature $\theta(\eta)$ and concentration $\phi(\eta)$ for different values of S. Both temperature and concentration increase with higher values of S. Additionally, slip impact facilitates better flow motion and heat dissipation compared to no-slip case (δ=β=0). Figures 3(a) and 3(b) depict the variations of the Brownian motion parameter (Nb) that affect the thermal $\theta(\eta)$ and concentration $\phi(\eta)$ fields. A notable rise in fluid temperature is observed with increasing Nb values, attributed to improved energy transport caused by the intensified motion and dispersing nanoparticles within the fluid. A similar trend is noticed in the case of nanoparticle concentration near the wall; this behavior results is noticed in Fig.3(b) from enhanced diffusion, which gives better heat and mass transport efficiency. Introducing slip conditions (δ=0.3, β=0.1) slightly reduces both thermal and nanoparticle concentration compared to the no-slip case (δ=β=0).

Figures 4(a), 4(b), and 4(c) depict the effects of velocity, temperature, and concentration profiles under varying values of the inclination parameter. In Figure 4(a), it is observed that the velocity field diminishes as the inclination increases, while the temperature and concentration profiles exhibit the opposite trend in Figures 4(b) and 4(c). It is evident that higher inclination angles of the magnetic field lead to a thickened momentum boundary layer. Consequently, it can be inferred that an increase in the magnetic field inclination parameter results in reduced fluid velocity and elevated fluid temperature and concentration within the boundary layer. The results also reveal that slip effects (δ=0.3, β=0.1) reduce the velocity, temperature, and concentration values compared to the no-slip case (δ=β=0), highlighting the significance of surface conditions in influencing transport phenomena. Figure 5 illustrates the effect of the thermophoresis parameter Nt on fluid temperature. Higher values of Nt are linked to an increase in fluid temperature. A rise in Nt encourages greater particle accumulation near the surface, which reduces the heat transfer rate and raises the temperature within the thermal boundary layer.

Figures 6(a), 6(b) and 6 (c) display the fluid velocity profile $f'(\eta)$, temperature profile $\theta(\eta)$ and concentration profile $\phi(\eta)$ for different values of thermal buoyancy parameter (λ) with the presence and absence of a magnetic field, respectively. In Fig.6(a), it is noticed that $f'(\eta)$ accelerates for growing values of λ due to enhanced buoyancy-driven flow, which promotes upward fluid motion. However, in the presence of a magnetic field (M=0.5), the opposing Lorentz force suppresses velocity, leading to lower shear stress at the wall. While the opposite trend has been observed both $\theta(\eta)$ and $\phi(\eta)$ for progressive values of λ is noticed in Fig.6(b)-(c), since stronger convective effects enhance thermal and species dissipation away from the surface.The effect of the chemical reaction parameter Kr on the concentration profile $\phi(\eta)$ is illustrated in Figure 7. It is noted that as the chemical reaction parameter Kr increases, the concentration profile $\phi(\eta)$ decreases. Physically, this occurs because a higher Kr accelerates the consumption of reactant species within the boundary layer, resulting in a reduced concentration near the surface. Additionally, it is noticed that the species concentration rises on enhancing the Lewis number Le.

Figures 8(a), 8(b), and 8(c) illustrate the fluid velocity profile, temperature profile, and concentration profile, respectively, for varying values of the Richardson number (Ri) under both slip and no-slip conditions. It is observed that the fluid velocity decreases as Ri values increase. Physically, a higher Ri indicates stronger buoyancy forces opposing the inertial flow, which leads to a slowdown in fluid motion and a reduction in velocity. However, this effect is moderated when slip parameters (δ, β) are introduced, which reduces flow resistance at the surface. Conversely, an opposite trend is evident in the temperature and concentration profiles with increasing Ri values. In these cases, both temperature and concentration are higher under no-slip conditions compared to slip conditions.

Figs. 9(a)-(e) display the ANN model's performance metric for estimating the engineering parameter skin friction in the presence of various values of mixed convection and magnetic fields. In this scenario, the ANN model achieves a minimal validation error with an MSE of 6.113e-10 at epoch 913. Additionally, it is noted that a high R value close to 1 indicates a strong correlation between the target and predicted values. In terms of physics, mixed convection modifies momentum transfer, which affects drag, while the magnetic field reduces velocity gradients near the surface, thereby decreasing skin friction. Similarly, this model demonstrates excellent validation performance with an MSE of 1.9755e-09 and 1.0253e-07 at epochs 1000 and 321, respectively. The error histogram shows a close concentration of error around zero, which indicates consistent and precise predictions for the Nusselt number and Sherwood number in the presence of (*M*, *Ec*) and (*Kr*, *s*), respectively. Additionally, the training state and regression plots illustrate the minimal validation checks and the strong predictive ability of the ANN model, as seen in Figs. 10(a)-(e) and 11(a)-(e).

Fig. 12 demonstrates the variation of the skin friction coefficient (*Cf*) for magnetic field (*M*) and mixed convection parameter (λ). It shows that increasing *M* leads to a slowdown of *Cf*, while a reverse trend is observed for increasing λ. This is because of the magnetic field's opposing Lorentz force, which slows down the fluid and reduces surface drag by reducing velocity gradients close to the surface. On the other hand, A rise in λ, indicates the influence of buoyancy and improves momentum transmission, which raises surface drag. According to these results, managing the magnetic field and mixed convection forces may be essential for applications like heat exchangers and MHD boundary layers, where reducing or increasing surface friction is required. Figure 13 illustrates the relationship between the Nusselt number (Nu) and the magnetic field (M) as well as the Eckert number (Ec). It shows that higher Ec, increases Nu, but decreases *Nu* for raising values of *M*. This is because a lower Nusselt number indicates that the magnetic field is dampening fluid motion, which lowers the rate of heat transfer at the surface. On the other hand, better thermal energy transmission results from a larger Eckert number, which enhances heat production through viscous dissipation. The Sherwood number (*Sh*)

varies with the Stefan blowing parameter (S) and the chemical reaction parameter (*Kr*), as seen in Fig.14. It was discovered that the enhanced values of S and *Kr* both cause *Sh* to rise. A greater chemical reaction parameter increases the concentration gradient, which speeds up mass diffusion and improves mass transfer at the surface, leading to a higher Sh. Additionally, by decreasing the thickness of the mass boundary layer, the Stefan blowing effect (S), which symbolizes the influence of surface blowing or suction on mass transfer, raises *Sh*.

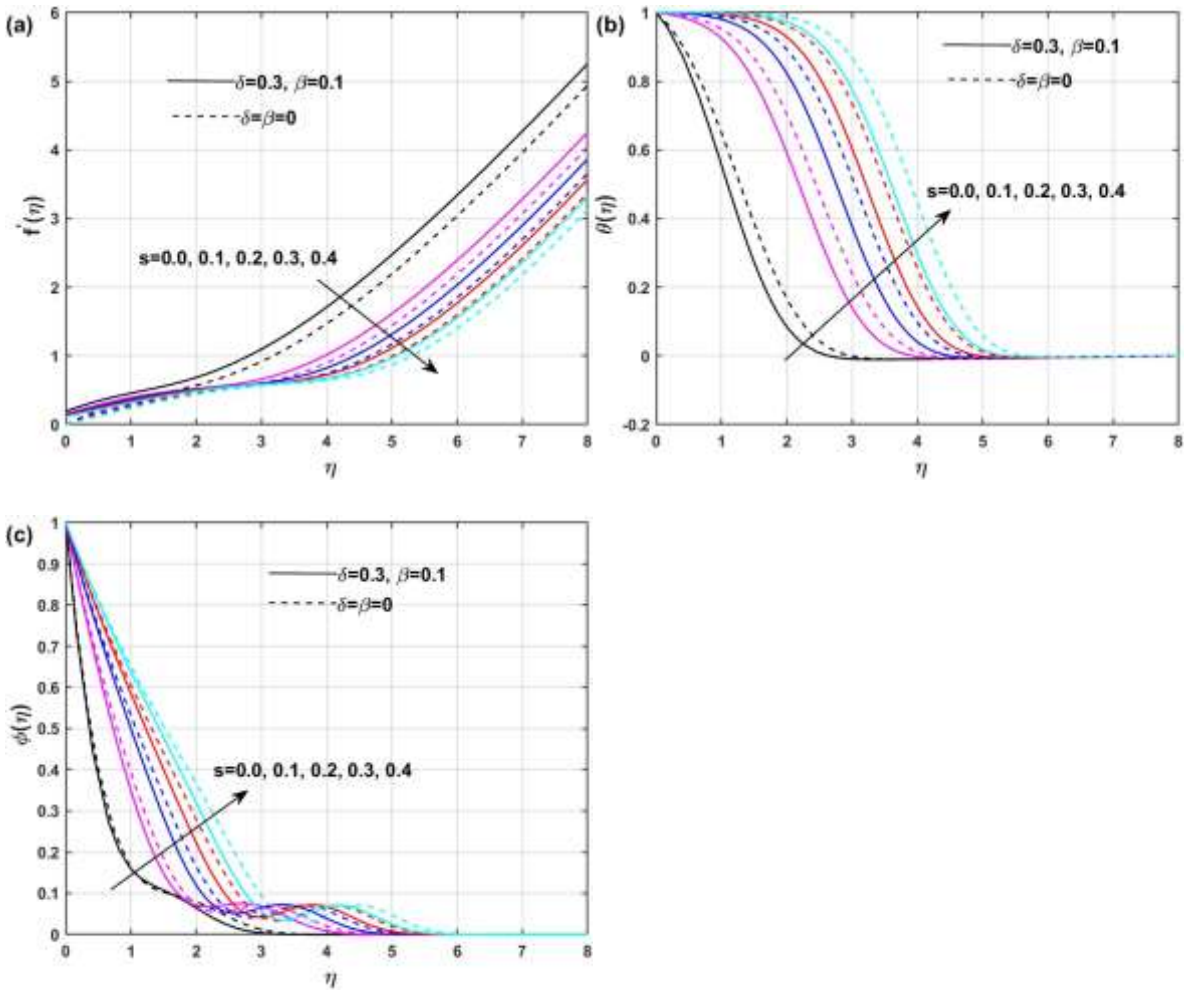

Figure 2. Effect of slip parameter ss on velocity, temperature, and concentration profiles for δ=0.3 and β=0.1.

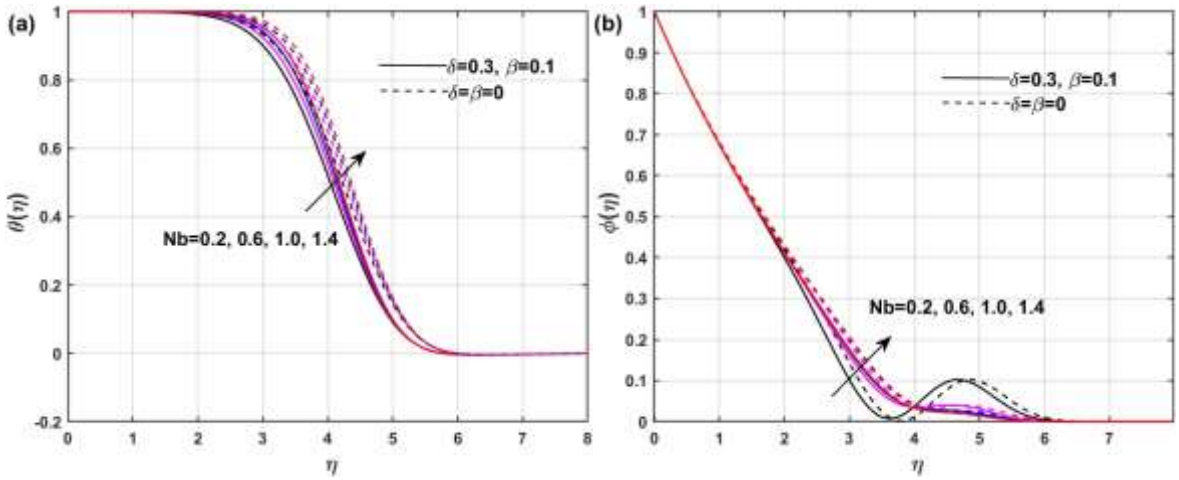

Figure 3. Effect of the Brownian motion parameter (Nb) on temperature and concentration profiles under slip and no-slip boundary conditions.

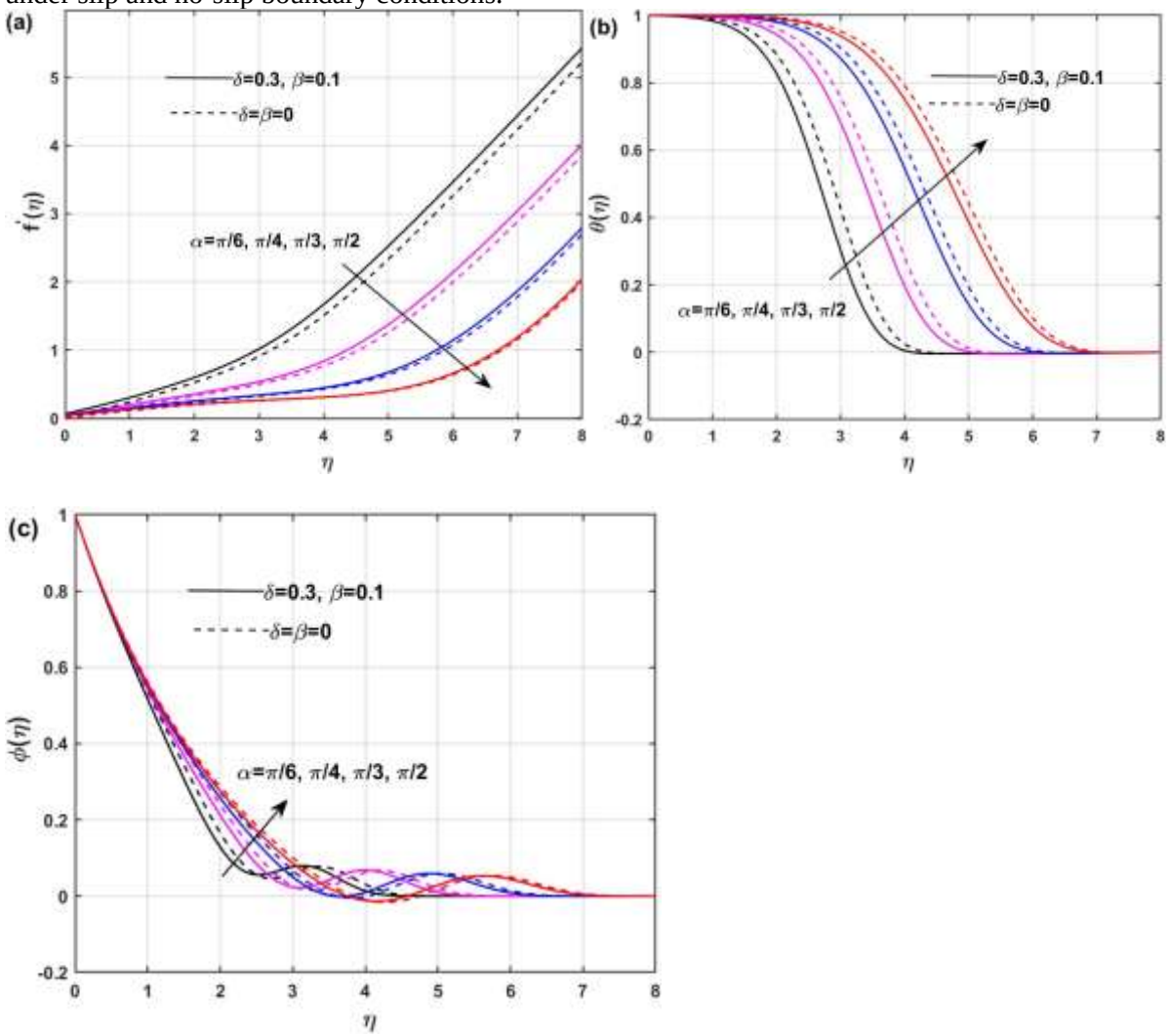

Figure 4. Effect of inclination angle (α) on velocity, temperature, and concentration profiles under slip and no-slip boundary conditions.

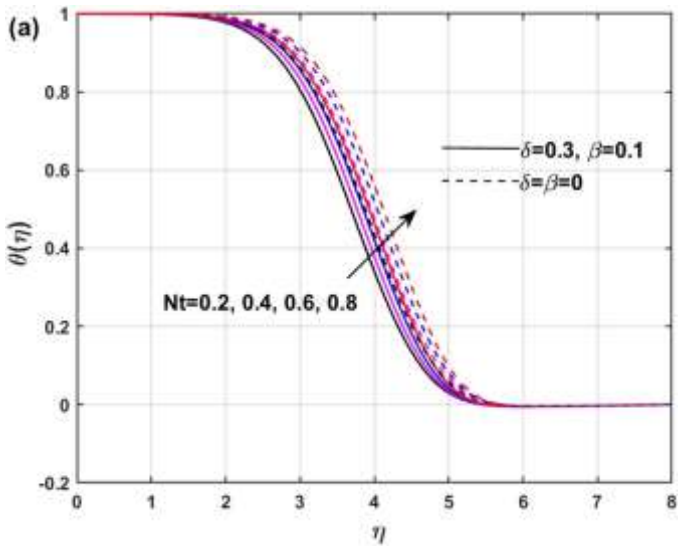

Figure 5. Effect of thermophoresis (Nt) on temperature and concentration profiles under slip and no-slip boundary conditions.

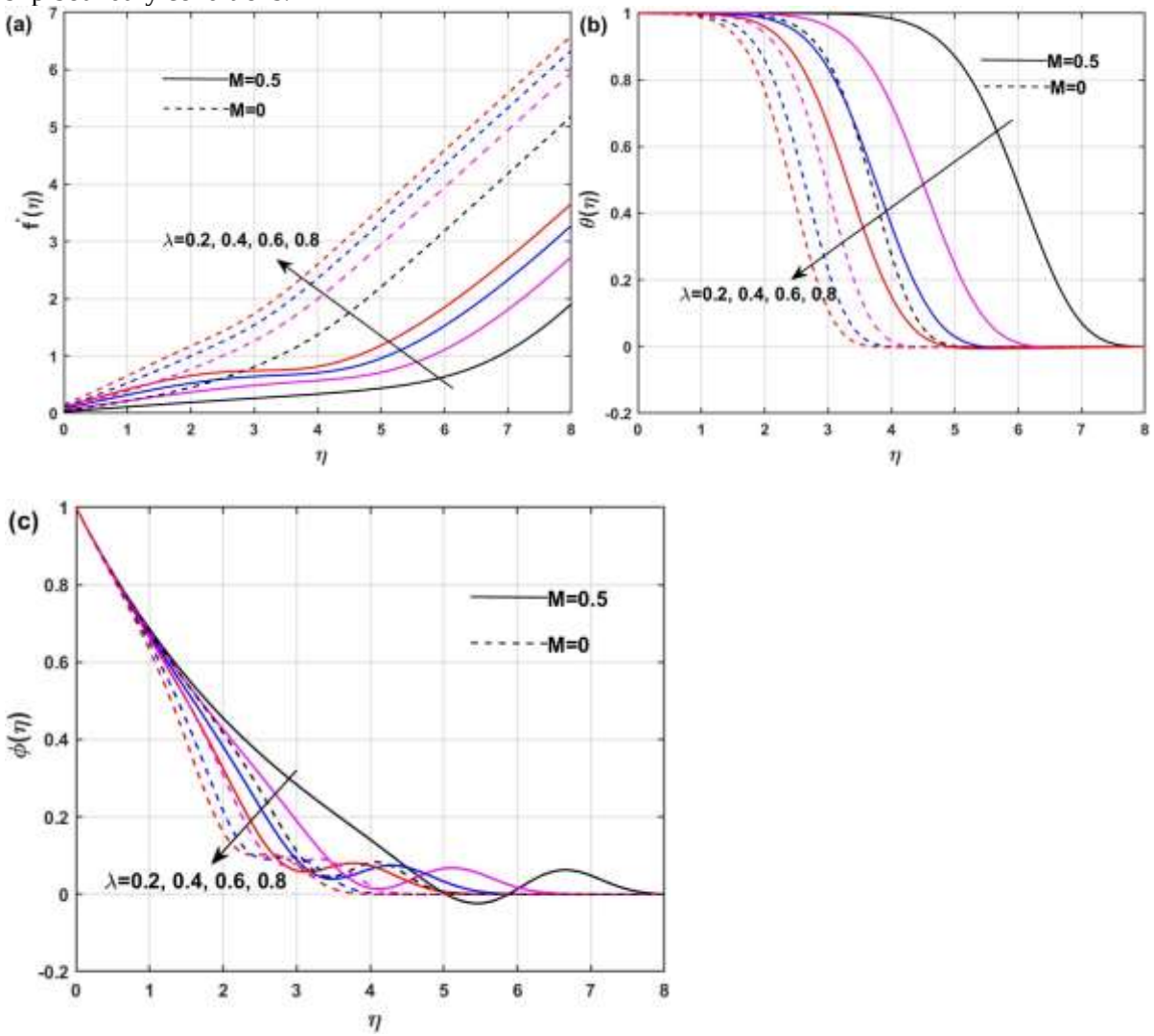

Figure 6. Effect of mixed convection parameter (λ) and magnetic field (M) on velocity, temperature, and concentration profiles.

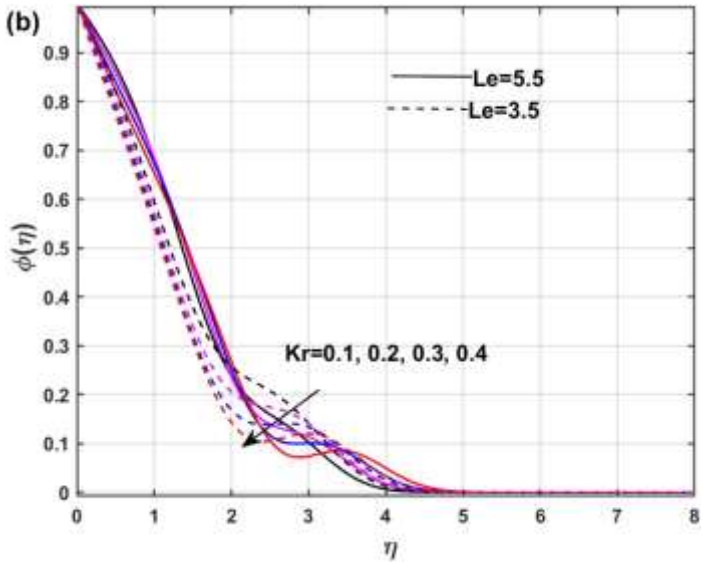

Figure 7. Effect of chemical reaction (Kr) and Lewis number (Le) on concentration profile.

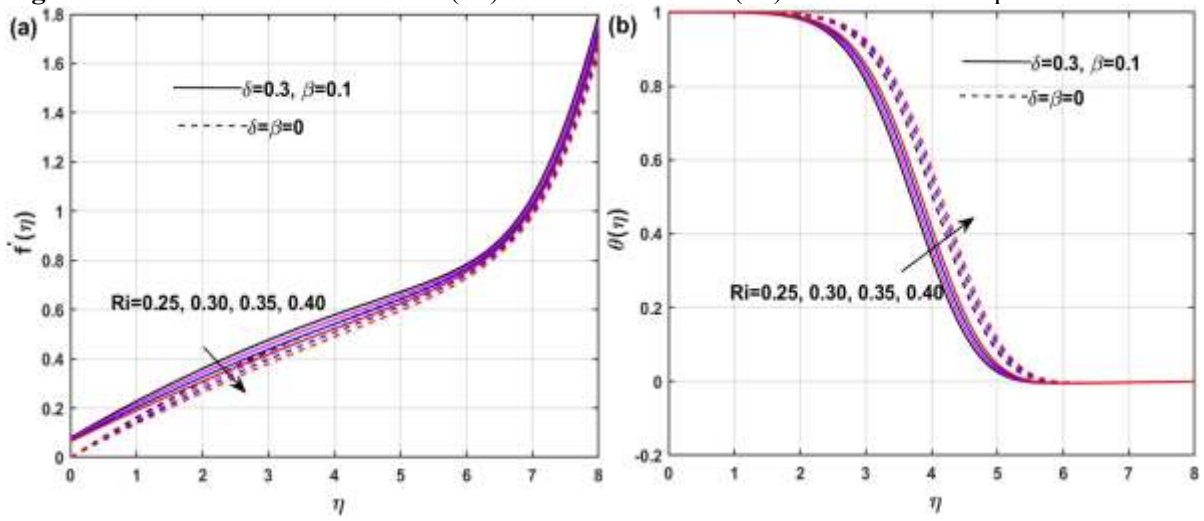

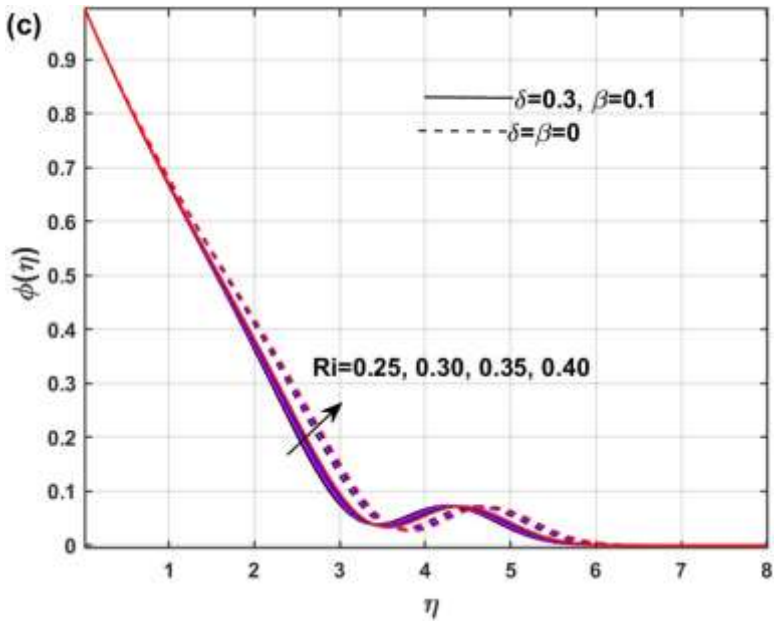

Figure 8. Effect of Richardson number parameter and magnetic field (M) on velocity, temperature, and concentration profiles under slip and no-slip boundary conditions

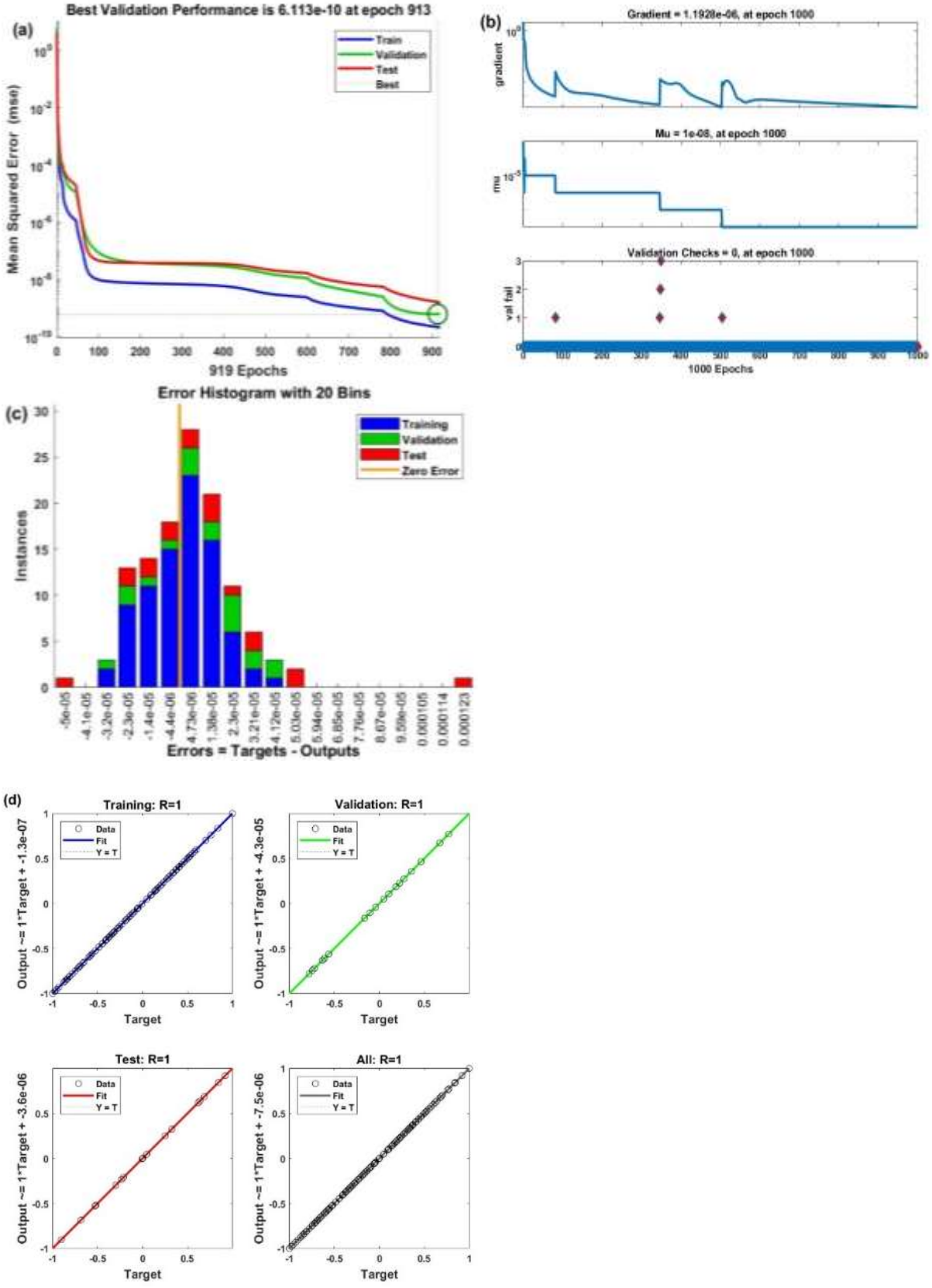

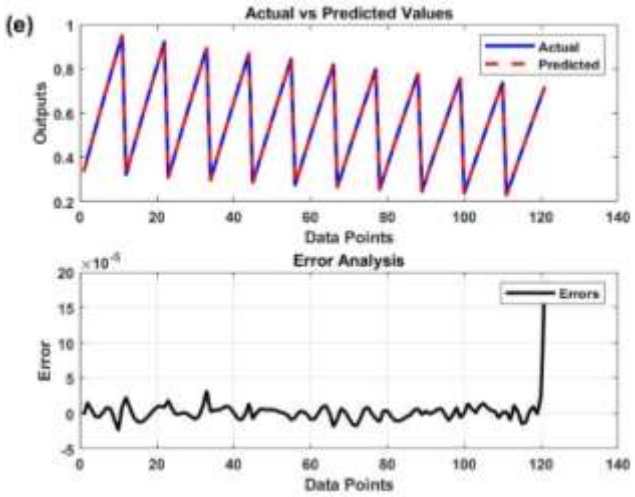

Figure 9. Variation of magnetic field(M) and mixed convection parameter (λ) (a) performance (b)Training state (c) Error Histogram (d)regression (e) error analysis for data points via ANN plots.

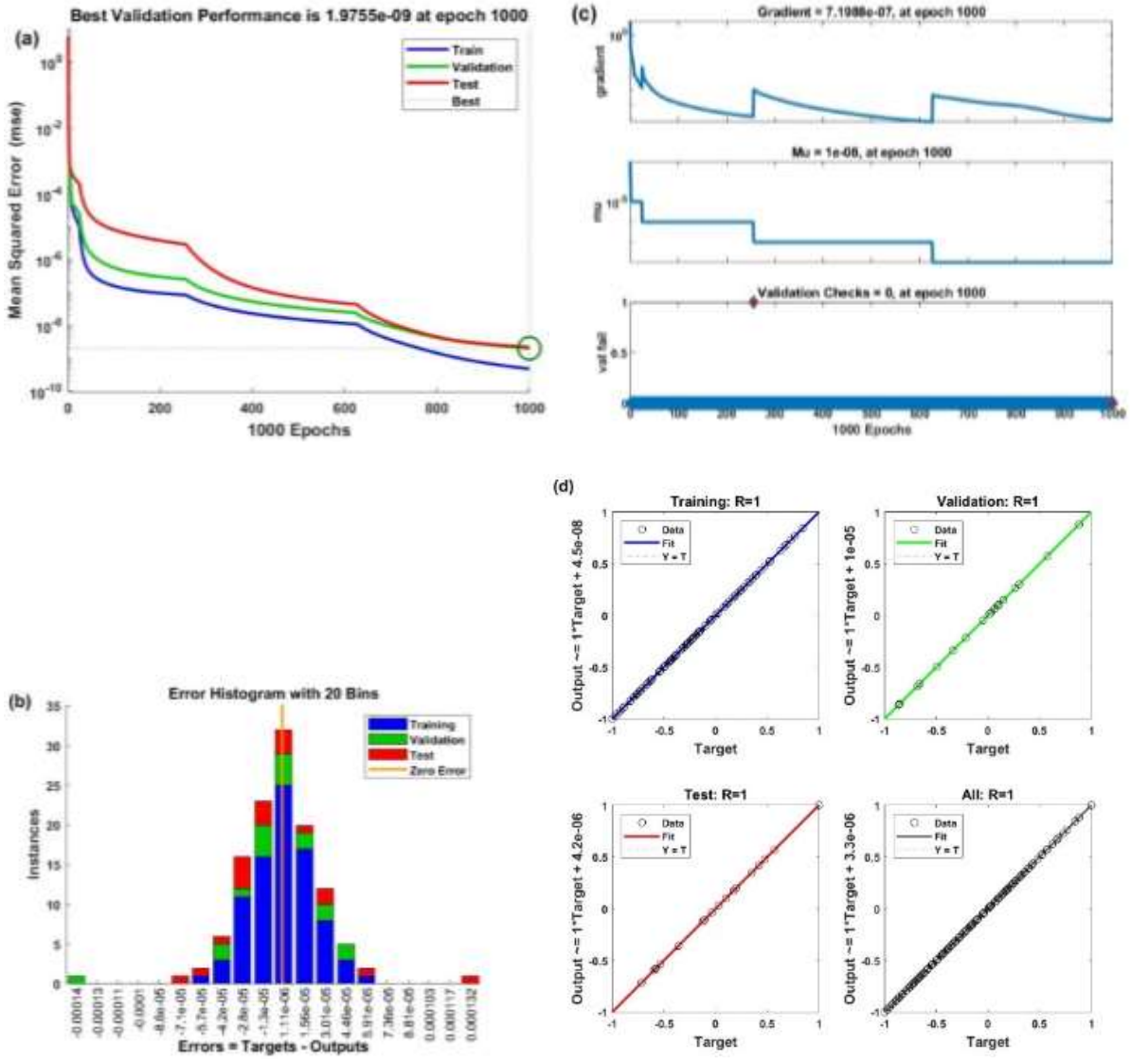

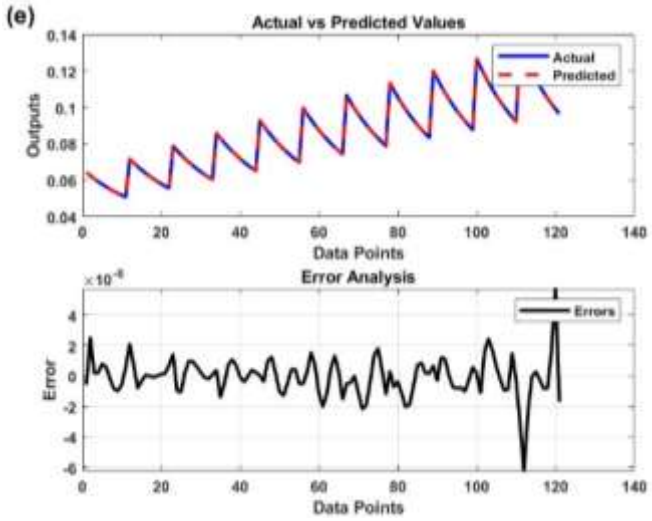

Figure 10. Variation of magnetic field (M) and Eckert number(Ec) against Nusselt number (a) performance (b)Training state (c) Error Histogram (d)regression (e) error analysis for data points via ANN plots.

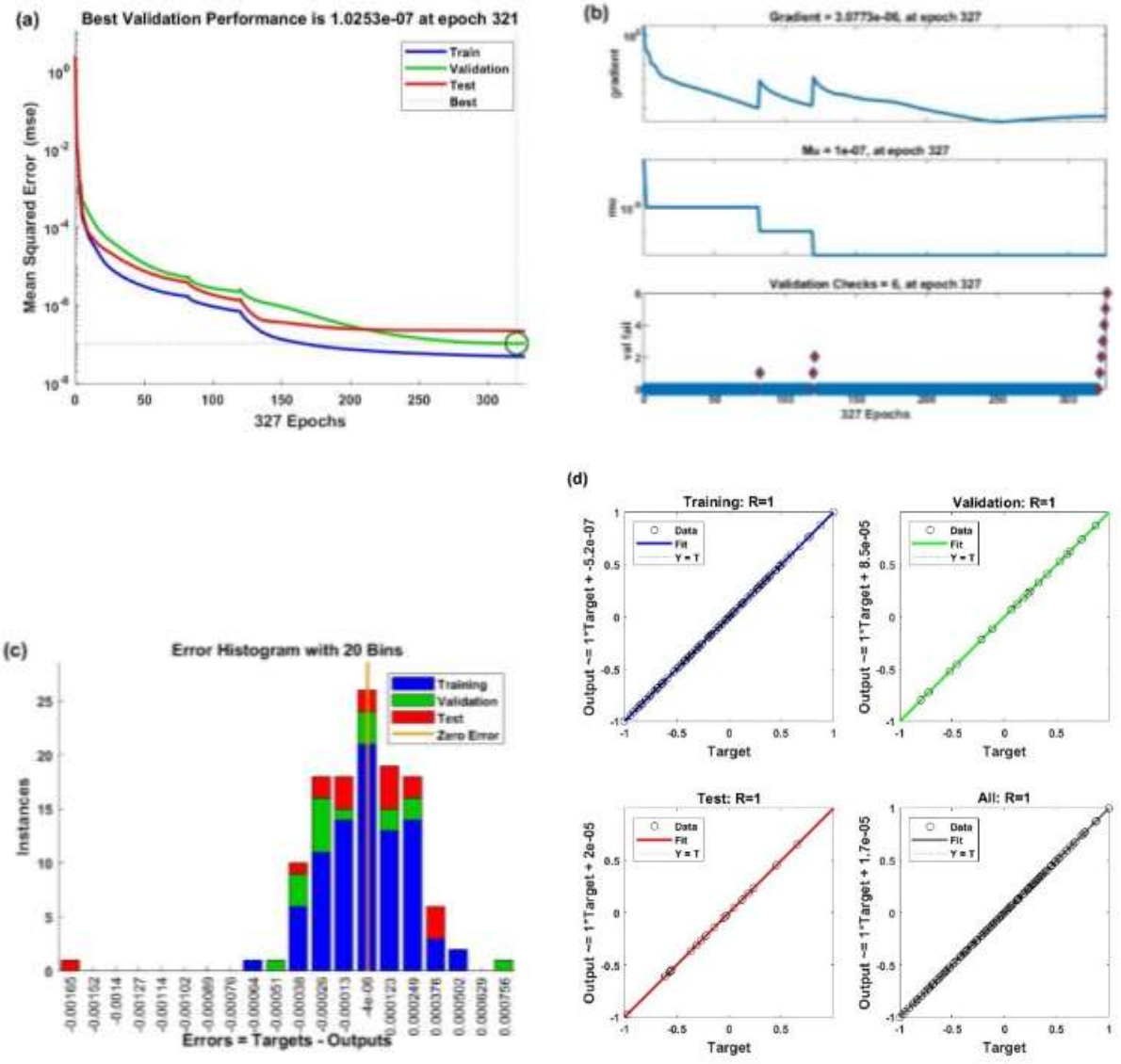

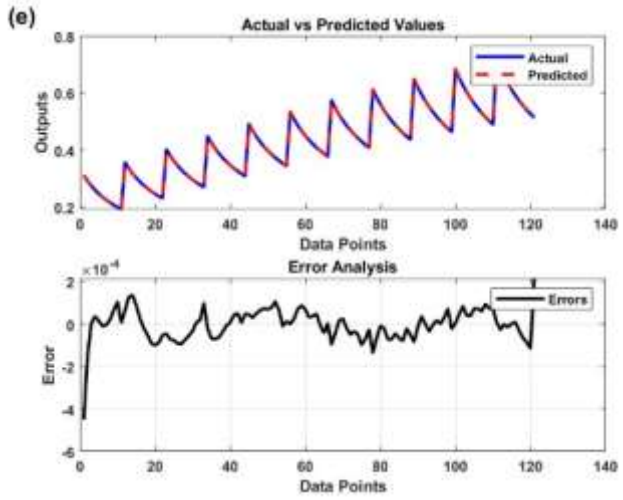

W

Figure 11. Variation of chemical reaction parameter (Kr) and Stefan blowing parameter (s) against Sherwood number (a) performance (b)Training state (c) Error Histogram (d)regression (e) error analysis for data points via ANN plots

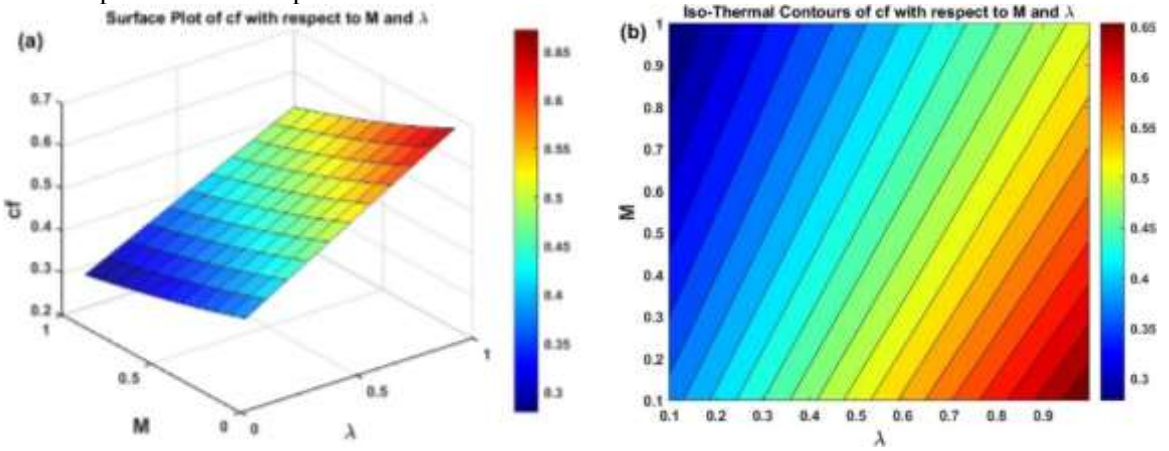

Figure 12. Impact of M and λ against Cf (a) surface plot (b) Contour Plot

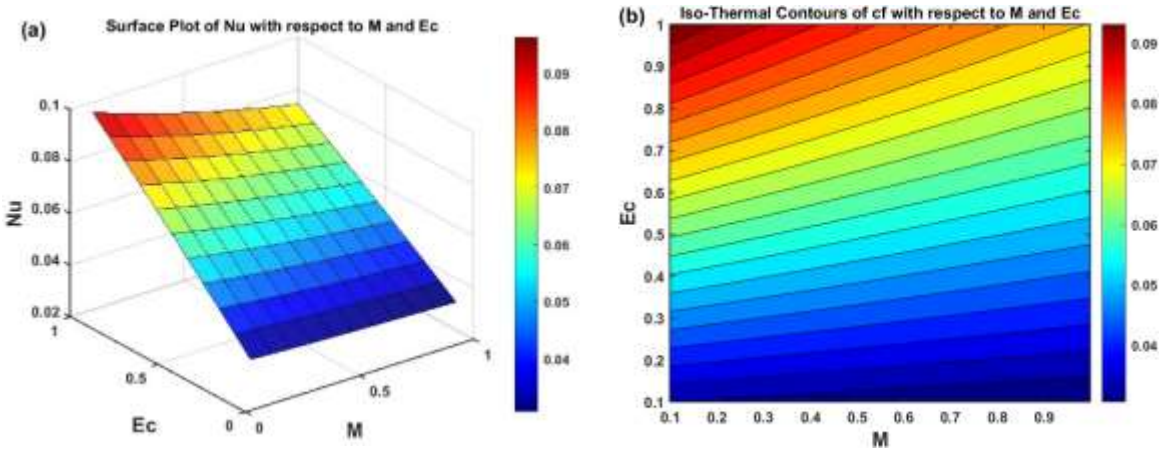

Figure 13. Impact of M and Ec against Nu (a) surface plot (b) Contour Plot

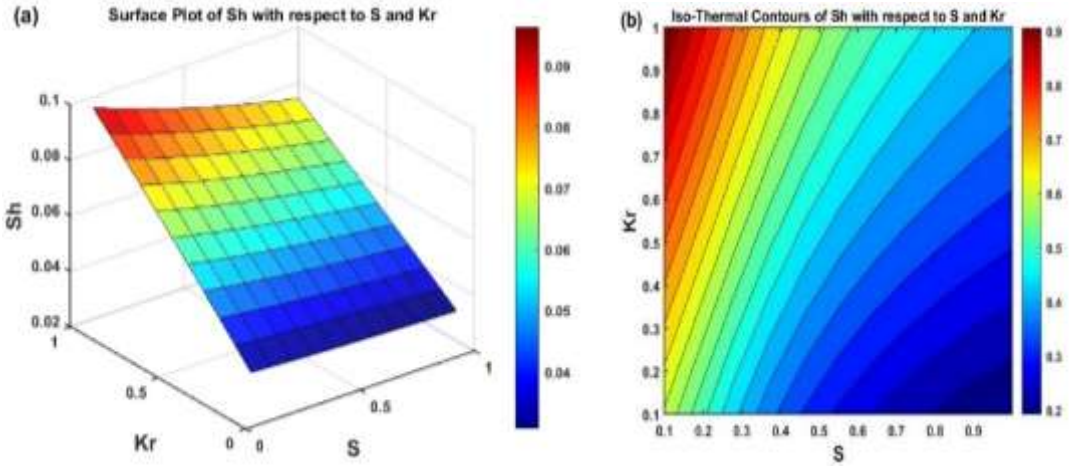

Figure 14. Impact of Kr and S against Sh (a) surface plot (b) Contour Plot

CONCLUSIONS

The hybrid computational analysis of the interaction among momentum, heat, and mass transfer in boundary layer flows over a chemically reactive magnetised nanofluid, incorporating Thomson-Troian slip and Stefan blowing effects, is presented. The main conclusions are summarised as follows:

- Stefan blowing considerably reduces fluid velocity but enhances both temperature and concentration in the boundary layer.
- Thompson–Troian slip conditions improve thermal control by reducing skin friction and suppressing velocity, temperature, and concentration profiles. At the same time, inclined magnetic fields (M) increase temperature and concentration layers while decreasing skin friction and velocity through the Lorentz force.
- Brownian motion (*Nb*) and thermophoresis (*Nt*) amplify thermal and solutal transport by increasing nanoparticle diffusion close to the surface.
- Mixed convection (λ) increases momentum transfer, enhancing skin friction and surface drag, whereas chemical reaction parameter (*Kr*) reduces the nanoparticle concentration by increasing reactant consumption.
- ANN modeling confirms the resilience of the model for real-world applications by achieving very accurate predictions of skin friction (MSE = 6.113×10^{-10}), Nusselt, and Sherwood numbers.

These results offer important new information for improving MHD boundary layer flows in chemical processing, heat exchangers, and industrial cooling. While the strong ANN models provide for accurate predictions for system design and performance improvement, the interaction of buoyancy effects, magnetic fields, and slip conditions presents potential for precise control of drag, heat, and mass transfer.

REFERENCES

1. Choi S.U., Eastman J.A. Enhancing thermal conductivity of fluids with nanoparticles (No. ANL/MSD/CP-84938; CONF-951135-29). *Argonne National Laboratory*. 1995.
2. Das S.K., Putra N., Thiesen P., Roetzel W. Temperature dependence of thermal conductivity enhancement for nanofluids. *Journal of Heat Transfer*. 2003; 125 (4): 567–574.
3. Buongiorno J. Convective transport in nanofluids. *Journal of Heat Transfer*. 2006; 128 (3): 240–250.
4. Eastman J.A., Choi S.U.S., Li S., Yu W., Thompson L.J. Anomalously increased effective thermal conductivities of ethylene glycol-based nanofluids containing copper nanoparticles. *Applied Physics Letters*. 2001; 78 (6): 718–720.
5. Xuan Y., Li Q. Heat transfer enhancement of nanofluids. *International Journal of Heat and Fluid Flow*. 2000; 21 (1): 58–64.

6. Yu W., Choi S.U.S. The role of interfacial layers in the enhanced thermal conductivity of nanofluids: a renovated Hamilton–Crosser model. *Journal of Nanoparticle Research*. 2004; 6: 355-361.
7. Habibishandiz M., Saghir M.Z. A critical review of heat transfer enhancement methods in the presence of porous media, nanofluids, and microorganisms. *Thermal Science and Engineering Progress*. 2022; 30: 101267.
8. Ikeda T., Kobayashi Y., Yamakawa M. Effect of Janus balance on the thermal conductivity of nanofluid. *Chemical Physics Letters*. 2025; 141969.
9. Hasan M.M., Rahman M.M., Rahman M.A., Bakar S.A., Islam M.S., Khalifa T. Artificial intelligent model to enhance thermal conductivity of TiO 2-Al 2 O 3/water-ethylene glycol-based hybrid nanofluid for automotive radiator. *IEEE Access*. 2024.
10. Banisharif A., Estellé P., Rashidi A., Van Vaerenbergh S., Aghajani M. Heat transfer properties of metal, metal oxides, and carbon water-based nanofluids in the ethanol condensation process. *Colloids and Surfaces A: Physicochemical and Engineering Aspects*. 2021; 622: 126720.
11. Kandasamy R., Loganathan P., Puvi Arasu P. Scaling group transformation for MHD boundary-layer flow of a nanofluid past a vertical stretching surface in the presence of suction/injection. *Nuclear Engineering and Design*. 2011; 241 (6): 2053–2059.
12. Yadav D., Bhargava R., Agrawal G.S. Boundary and internal heat source effects on the onset of Darcy–Brinkman convection in a porous layer saturated by nanofluid. *International Journal of Thermal Sciences*. 2012; 60: 244-254.
13. Zikanov O., Listratov Y.I., Sviridov V.G. Natural convection in horizontal pipe flow with a strong transverse magnetic field. *Journal of Fluid Mechanics*. 2013; 720: 486-516.
14. Ibrahim W. Magnetohydrodynamic (MHD) boundary layer stagnation point flow and heat transfer of a nanofluid past a stretching sheet with melting. *Propulsion and Power Research.* 2017; 6 (3): 214-222.
15. Daniel Y.S., Aziz Z.A., Ismail Z., Bahar A., Salah F. Stratified electromagnetohydrodynamic flow of nanofluid supporting convective role. *Korean Journal of Chemical Engineering.* 2019; 36: 1021-1032.
16. Arshad M. MHD hybrid nanofluid flow in a rotating system with an inclined magnetic field and thermal radiation. *Case Studies in Thermal Engineering*. 2024; 62: 105182.
17. Hussain Z., Nauman A., Ali M., Khan W.A., Alaoui M.K., Mazahirul I. Stability analysis of MHD thermo-capillary hybrid nanofluids in cylindrical flow within a porous medium. *International Journal of Heat and Fluid Flow*. 2025; 112: 109718.
18. Lakshmi C.V., Aravapalli A., Venkatadri K., Öztop H.F. Artificial Neural Network-Based Parameter Estimation in Lattice Boltzmann Simulations of MHD Nanofluid Natural Convection with Oscillating Wall Temperature. *Computers & Mathematics with Applications*. 2026; 205: 40-62.
19. Aydın O., Kaya A. MHD mixed convection of a viscous dissipating fluid about a permeable vertical flat plate. *Applied Mathematical Modelling*. 2009; 33 (11): 4086-4096.
20. Raza Q., Ali B., Ghazwani H.A., Younis J. ANN-based modeling of porous MHD mixed convection in tri-hybrid nanofluids with thermal radiation. *Journal of Radiation Research and Applied Sciences*. 2025; 18 (3): 101852.
21. Potla R.T., Abbas Z., Alqahtani N.A., Arslan M.S. Regression analysis for thermal transport of cilia-driven MHD Sutterby liquid under joule heating and heat sink/source using ANN. *Case Studies in Thermal Engineering*. 2025; 107320.
22. Ishaq M., Ashraf M.B., Hamzi A.M., Altherwi A.A., Alshehery S., Jari H. Intelligent computing of mixed convection Casson fluid flow with microrotation effects using neural network backpropagation. *International Communications in Heat and Mass Transfer*. 2026; 171: 110079.
23. Lakshmi C.V., Aravapalli A., Venkatadri K., Öztop H.F. Artificial Neural Network-Based Parameter Estimation in Lattice Boltzmann Simulations of MHD Nanofluid Natural Convection

with Oscillating Wall Temperature. *Computers & Mathematics with Applications*. 2026; 205: 40-62.
24. Thompson P.A., Troian S.M. A general boundary condition for liquid flow at solid surfaces. *Nature*. 1997; 389 (6649): 360-362.
25. Tretheway D.C., Meinhart C.D. Apparent fluid slip at hydrophobic microchannel walls. *Physics of Fluids*. 2002; 14 (3): L9-L12.
26. Turkyilmazoglu M. Multiple solutions of heat and mass transfer of MHD slip flow for the viscoelastic fluid over a stretching sheet. *International Journal of Thermal Sciences*. 2011; 50 (11): 2264-2276.
27. Haq R.U., Nadeem S., Khan Z.H., Noor N.F.M. Convective heat transfer in MHD slip flow over a stretching surface in the presence of carbon nanotubes. *Physica B: Condensed Matter*. 2015; 457: 40-47.
28. Reddy K.M., Kaladhar K., Srinivasacharya D. Influence of inclined magnetic field, radiation, and Hall current on mixed convection flow through an inclined channel with Navier-slip condition. *Journal of Applied Nonlinear Dynamics*. 2022; 11 (02): 271-282.
29. Mohanaphriya U., Chakraborty T. Entropy optimization in a radiative and chemically reactive EMHD flow of a nanofluid coexisting Ohmic dissipation and multiple slips. *International Journal of Numerical Methods for Heat & Fluid Flow*. 2024; 34 (12): 4462-4519.
30. Algarni A. Enhanced heat transport analysis in non-Newtonian chemically reactive hybrid nanofluid flow over a cylindrical geometry subjected to Thompson and Troian slip consequences. *Journal of Radiation Research and Applied Sciences*. 2025; 18 (1): 101263.
31. Mukhopadhyay S. Slip effects on MHD boundary layer flow over an exponentially stretching sheet with suction/blowing and thermal radiation. *Ain Shams Engineering Journal*. 2013; 4 (3): 485-491.
32. Gowda R.P., Kumar R.N., Prasannakumara B.C., Nagaraja B., Gireesha B.J. Exploring magnetic dipole contribution on ferromagnetic nanofluid flow over a stretching sheet: An application of Stefan blowing. *Journal of Molecular Liquids*. 2021; 335: 116215.
33. Punith Gowda R.J., Baskonus H.M., Naveen Kumar R., Prasannakumara B.C., Prakasha D.G. Computational investigation of Stefan blowing effect on flow of second-grade fluid over a curved stretching sheet. *International Journal of Applied and Computational Mathematics*. 2021; 7 (3): 109.
34. Joyce M.I., Kandasamy J., Sivanandam S. Effects of Stefan blowing and double stratification on convective hybrid nanoliquid flow with convective boundary and entropy generation. *Multidiscipline Modeling in Materials and Structures*. 2025.
35. Turkyilmazoglu M. Exact analytical solutions for heat and mass transfer of MHD slip flow in nanofluids. *Chemical Engineering Science*. 2012; 84: 182-187.
36. Albaqami NN. Using artificial neural network analysis to study Jeffrey nanofluid flow in cone–disk systems. *Mathematical and Computational Applications*. 2024; 29 (6): 98.
37. Abdal S, Taha T, Ali L, Zulqarnain RM, Yook SJ. Neural networking-based approach for examining heat transfer and bioconvection in Non-Newtonian fluid with chemical reaction over a stretching sheet. *Case Studies in Thermal Engineering*. 2025; 69: 106047.
38. Shettar M, Bhat A, Katagi NN, Gowrishankar MC. Experimental Investigation on Mechanical Properties of Glass Fiber–Nanoclay–Epoxy Composites Under Water-Soaking: A Comparative Study Using RSM and ANN. *Journal of Composites Science*. 2025; 9 (4): 195.
39. Arunachalam SJ, Saravanan R, Sathish T, Alarfaj AA, Giri J, Kumar A. Enhancing mechanical performance of MWCNT filler with jute/kenaf/glass composite: a statistical optimization study using RSM and ANN. *Materials Technology*. 2024; 39 (1): 2381156.

